



Fingerprint-shaped triboelectric tactile sensor

Xuecheng Qu^{a,c}, Jiangtao Xue^{a,d}, Ying Liu^{a,c}, Wei Rao^{f,*}, Zhuo Liu^{a,b,**}, Zhou Li^{a,c,e,g,**}

^a CAS Center for Excellence in Nanoscience, Beijing Key Laboratory of Micro-nano Energy and Sensor, Beijing Institute of Nanoenergy and Nanosystems, Chinese Academy of Sciences, Beijing 101400, China

^b Key Laboratory of Biomechanics and Mechanobiology, Ministry of Education, Beijing Advanced Innovation Center for Biomedical Engineering, School of Biological Science and Medical Engineering, Beihang University, Beijing 100191, China

^c School of Nanoscience and Technology, University of Chinese Academy of Sciences, Beijing 100049, China

^d School of Life Science, Institute of Engineering Medicine, Beijing Institute of Technology, Beijing 100081, China

^e Center of Nanoenergy Research, School of Physical Science and Technology, Guangxi University, Nanning 530004, China

^f CAS Key Laboratory of Cryogenics, Technical Institute of Physics and Chemistry, Chinese Academy of Sciences, Beijing 100190, China

^g Institute for Stem Cell and Regeneration, Chinese Academy of Sciences, Beijing 100101, China

ARTICLE INFO

Keywords:

Fingerprint-shaped
Triboelectric nanogenerator
Liquid metal
Tactile sensor
Multifunctional

ABSTRACT

Tactile perception sensing, which could endow artificial devices with human-like abilities, is indispensable for new generation intelligent prosthetic. However, the development of flexible tactile sensors with multifunctional capabilities and low power consumption that remains an on-going challenge. Here, we purpose a flexible fingerprint-shaped triboelectric tactile sensor (FTTS) using eutectic gallium-indium (EGaIn) liquid metal and silicone. Based on the principle of triboelectric nanogenerator, the fabricated FTTS is composed of three independent fingerprint-like channels for liquid metal filling, with contact separation and stretching working modes to accommodate different application scenarios. Due to the flexible multi fingerprint-shaped channel design and the principle of triboelectricity, the FTTS has a fast response speed of 1.01 ms, and lower detection limit, which could stretch up to 225%. The fabricated FTTS is capable of pressure intensity and position detection, password simulation, material identification and pulse monitoring. In addition, this active sensor could realize zero power consumption of the sensing part without external power supply needed. The tactile perception and simulation technology based on this triboelectric sensing will definitely show broad prospects in the fields of intelligent prosthetics, medical rehabilitation and human-computer interaction.

1. Introduction

Tactile perception is one of the most essential ways for human beings to interact with the external environment [1]. Wearable tactile sensors, as a promising field have absorbed much attention, and have been widely used for artificial prosthetics, haptic perception, intelligent robotics, and other human-machine interaction applications, achieving several important functions like human tactile perception, such as contact force, temperature, humidity, and so on [2–7]. The principle of these kind of sensor are mainly based on capacitive, piezoresistive and piezoelectric [8–12]. As we know, human fingers are particularly sensitive to tactile perception. It is crucial to reconstruct these senses to provide the best replacement for upper limb amputees [13]. Due to the complex curved shape and limited installation space of prosthetic hands,

traditional tactile sensors may be too rigid to fit the irregular surface. In addition, the power consumption and sensitivity of the sensor are also urgent to be solved. So new requirements are put forward for these kinds of sensors.

The development of flexible and functional electronic materials has effectively promoted the revolution of this field. At present, silver nanowires, carbon nanotubes, hydrogels, and liquid metal have been reported for the structural design of tactile sensors [6,14,15]. Under normal circumstances (22 °C), liquid metal is in a liquid state and has high conductivity and fluidity, which can improve the durability and stability of the tactile sensor for long-term use [16,17]. Nowadays, a great body of research of finger-liked tactile sensor has focused on the piezoresistive based principle with liquid metal as the variable resistor. Some researchers proposed a highly stretchable liquid metal tactile

* Corresponding author.

** Corresponding authors at: CAS Center for Excellence in Nanoscience, Beijing Key Laboratory of Micro-nano Energy and Sensor, Beijing Institute of Nanoenergy and Nanosystems, Chinese Academy of Sciences, Beijing 101400, China

E-mail addresses: weirao@mail.ipc.ac.cn (W. Rao), liuzhuo@buaa.edu.cn (Z. Liu), zli@binn.cas.cn (Z. Li).

<https://doi.org/10.1016/j.nanoen.2022.107324>

Received 24 March 2022; Received in revised form 18 April 2022; Accepted 26 April 2022

Available online 29 April 2022

2211-2855/© 2022 Elsevier Ltd. All rights reserved.

sensor that integrated into the fingertip, demonstrating the feasibility of real-time slip detection and prevention of a grasped object [18]. And a research team proposed a 3D printed force tactile sensing based on liquid metal, which can accurately measure the temperature contact forces using in robotic manipulation [16]. However, the test process of the sensor based on piezoresistive principle is more complex, which requires special test circuit and signal amplifier, and it is easily affected by temperature. In addition, the sensitivity and lower limit of force detection need to be improved.

Coupling effects of triboelectrification and electrostatic induction, triboelectric nanogenerator could convert mechanical energy into electricity energy/electrical signal directly, without any complex signal acquisition equipment. Triboelectric nanogenerator as active sensor with characteristics of high sensitivity, reliable performance and high signal-to-noise ratio have been widely used in implantable medical device [19–24], intelligent robot [25–27], rehabilitation aids [28–32], and so on [33–38].

In this study, we develop a flexible fingerprint-shaped triboelectric tactile sensor (FTTS) using eutectic gallium-indium (EGaIn) and silicone

for multifunctional application. As a common liquid metal, EGaIn has the characteristics of low melting point, high surface tension, and good electrical conductivity, which is suitable as the stretchable electrode of the sensor. The patterned silicone is as the friction layer for enhancing the triboelectric charge density to improve both the output performance and sensitivity of the FTTS. The liquid metal is injected into the designed three independent fingerprint-shaped microfluidic channels with good stretchability. Based on the triboelectric nanogenerator principle, the FTTS is the coupling of contact separation and stretching working modes to cope with different application scenarios. Due to the FTTS's excellent sensitivity, fingerprint-like multi-channel design and triboelectric principle, it is ideal for applications such as pressure intensity and position detection, password simulation, materials identification, and pulse monitoring, which great promise in the field of intelligent prostheses, medical rehabilitation and human-machine interaction.

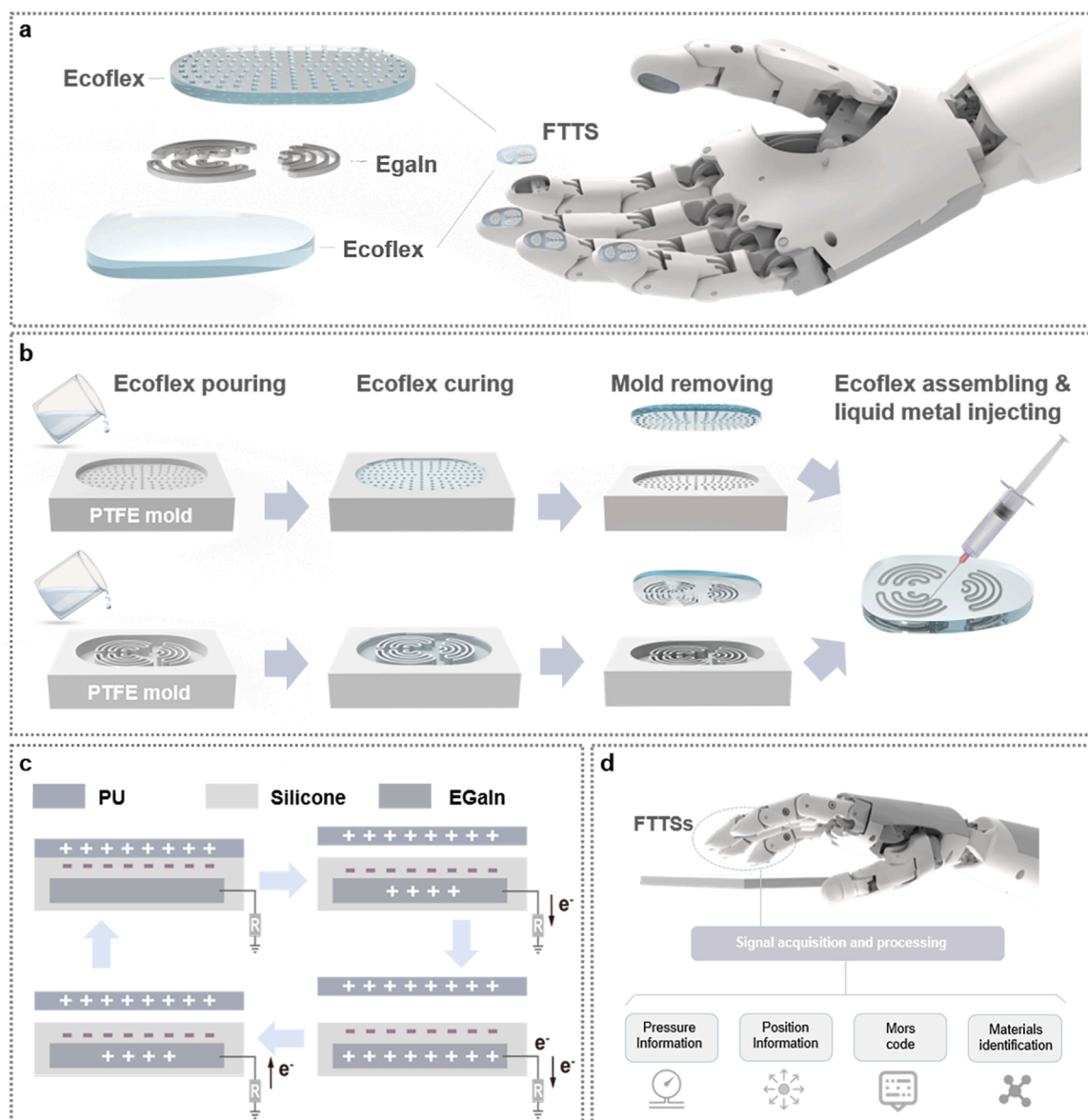


Fig. 1. Preparation process and principle of the FTTS. (a) Schematic structure of the FTTS, and the schematic diagram of the application with intelligent prosthesis. (b) The fabrication process of the FTTS. (c) Working principle of the FTTS in contact-separation mode. (d) Various application functions realized by the FTTS, such as pressure and position detection, Morse code and materials identification.

2. Results and discussion

2.1. Preparation process and principle of FTTS

FTTS is designed to be worn on the finger of the prosthetic and intelligent manipulator for obtaining various tactile information during touching applications (Fig. 1a and Fig. S1). This tactile sensor is mainly composed of two parts: silicone (Ecoflex 00–30) with micro-surface structure, and liquid metal (EGaIn) embedded in silicone channel. The channels inside the FTTS are arranged in three sets to form the fingerprint shape. To better fit the bionic fingertip, the overall width and length of the FTTS are set as 15 mm and 20 mm, respectively. The

fabricating process of the FTTS is shown in Fig. 1b. See the experimental section for detailed methods. The assembled device is approximately 3.3 mm thick.

To illustrate the operating mechanism of the FTTS with contact-separation mode, which in principle involves the combination effects of triboelectrification and electrostatic induction (Fig. 1c). The silicone is as the friction layer, and liquid metal is as electrode layer. In the initial state, the FTTS comes in contact with external contact layer (polyurethane (PU) film), the equal amounts of positive and negative charges are produced on the surface of PU and silicone due to the triboelectrification effect. When the FTTS begins to separate from PU, this equilibrium state is broken, so that the electrons flowed from the liquid

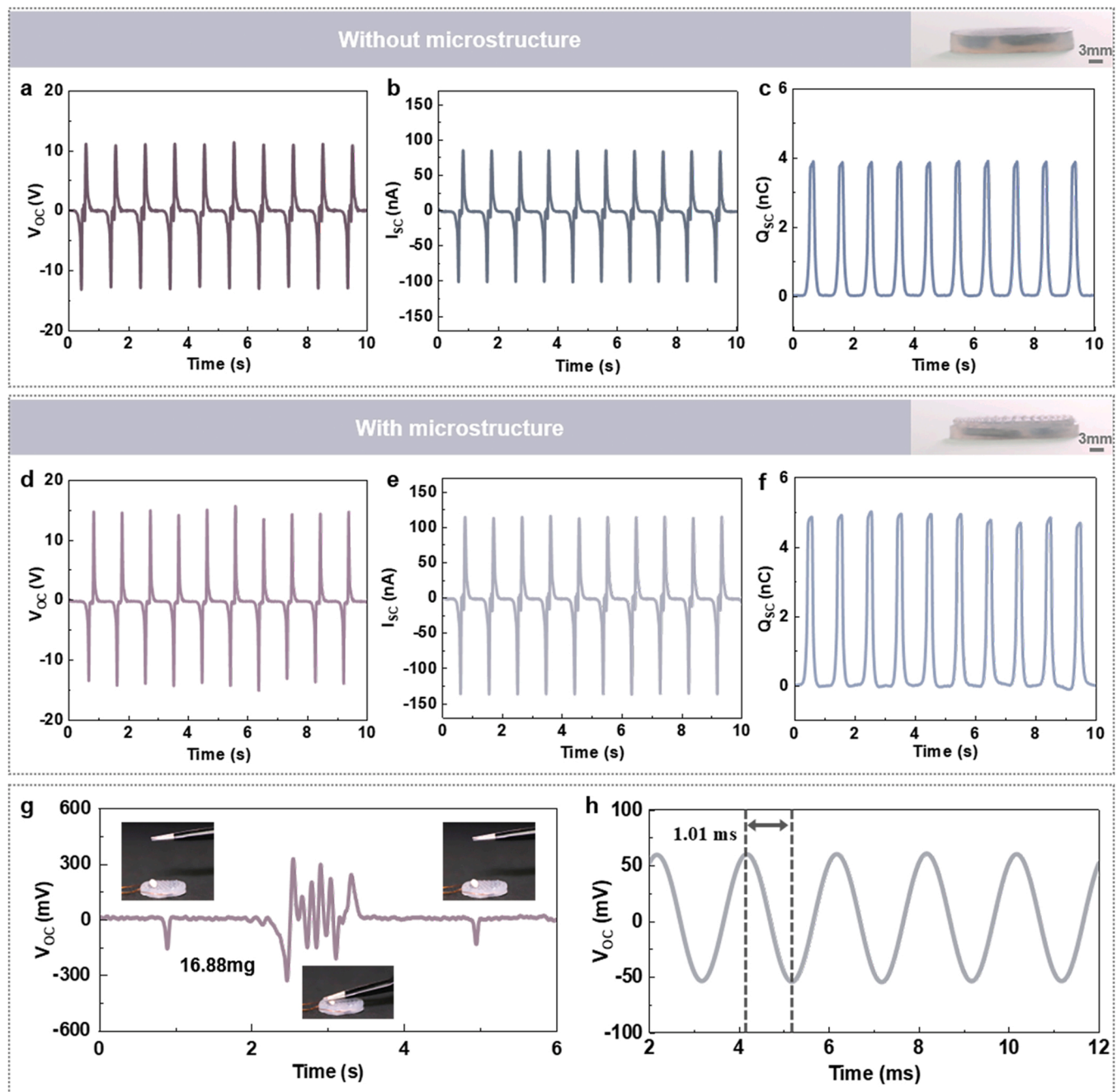


Fig. 2. Electrical output performance of the FTTS. (a-c) V_{OC} , I_{SC} and Q_{SC} of the FTTS without micro-surface structure progress on the surface of the silicone (contact and separated with PU, 1 Hz). (d-f) V_{OC} , I_{SC} and Q_{SC} of the FTTS with micro-surface structure progress on the surface of the silicone (contact and separated with PU, 1 Hz). (g) Sensitivity test of the FTTS for detecting a force as light as 16.88 mN equaling to the weight of a rice grain. (h) Response performance test of the FTTS under the frequency of 500 Hz.

metal electrode to the reference electrode (the ground) for a new balance, generating output signal based on electrostatic induction. The amplitude of this signal reaches the maximum value when they are completely separated. Then the FTTS approaches to the PU again, electrons flow from the ground to the liquid metal for rebalancing, producing a negative output signal. This is a full cycle based on this triboelectric sensing. The corresponding COMSOL simulation schematic diagram is shown in Fig. S2. By processing and analyzing the acquired signals, the fingerprint-shaped triboelectric tactile sensor could be used for a variety of applications such as pressure and position detection, materials identification, and so on (Fig. 1d).

2.2. Electrical output performance of the FTTS

Based on the above-mentioned working mechanism, the electrical output performance of the FTTS is systematically studied. Compared with the device without surface microstructure treatment, the output performance of the FTTS with micro-surface structure (hemispheres of 0.5 mm diameter) on the silicone surface has been significantly improved. As shown in Fig. 2a-f, the open circuit voltage (V_{OC}), short circuit current (I_{SC}) and transferred charge (Q_{SC}) are improved by about 36%, 28%, and 26%, respectively. After surface treatment for the silicone, the V_{OC} , I_{SC} , and Q_{SC} of the FTTS could reach at 15.3 V, 115.6 nA

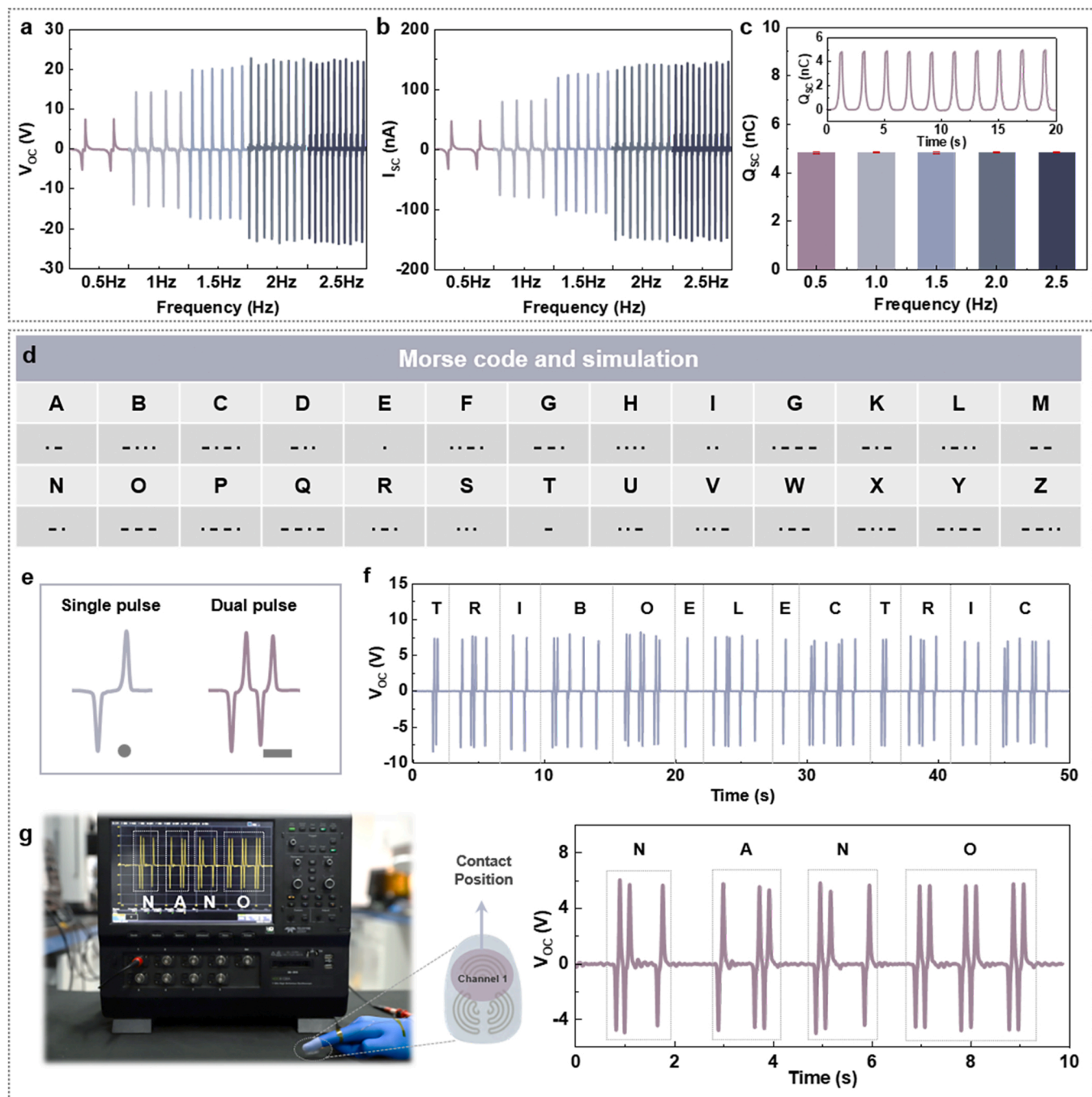


Fig. 3. Characterization of position signal and application of multi-channel information interaction of the FTTS. (a-c) V_{OC} , I_{SC} and Q_{SC} of the FTTS (with PU) at different contact and separation frequency (0.5 Hz, 1 Hz, 1.5 Hz, 2 Hz, and 2.5 Hz). (d) Part of Morse code. (e) Encode between the output signal of the FTTS and the input signal of Morse code. (f) The information simulation and identification of the strings "TRIBOELECTRIC" enabled by the FTTS. (g) The information simulation and identification of the strings "NANO" enabled by the FTTS.

and 5.1 nC, respectively. And The FTTS could effectively detect a force as light as 16.88 mN equaling to the weight of a rice grain, exhibiting good sensitivity and lower detection limit (Fig. 2g and Supplementary materials Video S1). Besides, the FTTS has a fast response speed of 1.01 ms (58.6 mV), ensuring accurate tactile information even with quick contact (Fig. 2h). To explore the water resistance of the FTTS, we soak the device in water for 48 h, and measure the VOC of the device before and after immersion. The results show that the output performance of the FTTS has no obvious attenuation after soaking in water, so that the FTTS has good water resistance (Fig. S3). In addition, the experimental data shows that temperature has no effect on the performance of the device in the range of 20–40 °C (Fig. S4).

Supplementary material related to this article can be found online at [doi:10.1016/j.nanoen.2022.107324](https://doi.org/10.1016/j.nanoen.2022.107324).

2.3. Frequency, fatigue test and application of single-channel information interaction of the FTTS

Further, the electrical output performance with different contact and separation frequency (0.5 Hz, 1 Hz, 1.5 Hz, 2 Hz, and 2.5 Hz) between FTTS and PU is also measured. As shown in Fig. 3a and Fig. 3b, within a certain range of 0.5–1 Hz, V_{OC} and I_{SC} are positively correlated with the test frequency. While it has little effect on V_{OC} and I_{SC} , when the frequency exceeded 1 Hz. In addition, Q_{SC} depends very little on the test frequency (Fig. 3c).

Morse code is an on-off signal code that expresses different character information through different sequences. It can be used in the fields of telegraphy, military, emergency rescue and so on, with good confidentiality and controllability. As shown in Fig. 3d, the 26 letters are represented by a short dot signal "." and a long signal "-", which could be replaced by single pulse and dual pulses from the FTTS when contacting any object surface, respectively, thanks to the sensor's high sensitivity and fast responsiveness (Fig. 3e). Here, combined with the encoding of the FTTS and Morse code, the information simulation and identification of the strings "TRIBOELECTRIC" (Fig. 3f) and "NANO" (Fig. 3g and Supplementary materials Video S2) are realized. With the FTTS, information interaction could be achieved anywhere by finger (or prosthetic) without complex mechanical equipment.

Supplementary material related to this article can be found online at [doi:10.1016/j.nanoen.2022.107324](https://doi.org/10.1016/j.nanoen.2022.107324).

In addition, during the experiment, we find that the FTTS has different output responses to different materials. Further, to investigate the ability of the FTTS to discriminate different material types, five different materials (PTFE, PS, Acrylic, Glass, and PA66) are as the test objects. As shown in Fig. S5, whether it is V_{OC} , I_{SC} , or Q_{SC} , the amplitude of the output signal with PTFE is always the weakest, and the direction is opposite to that of other materials. In addition, the output signals of the FTTS with PS, acrylic, glass and PA66 show an upward trend, and the signal direction remains consistent. The small Figures in Fig. S5a and Fig. S5b are enlarged views of PTFE and PS output signals, respectively. By reason that, according to triboelectric series, PA66 possesses the strongest electropositivity, then Glass, Acrylic PS, and PTFE. In the contact-separation mode, the stronger the difference in electropositivity (or electronegativity) between the external material and the FTTS silicone layer, the more obvious the output amplitude, and the direction of the output signal is divided into positive and negative, which providing the possibility for smart manipulators or prostheses to realize function of materials identification.

The fatigue test of the FTTS is also conducted under the continuous 1 Hz mechanical impact, as shown in Fig. S6, which indicates that the V_{OC} has no obvious attenuation after 20, 000 cycles of testing compared with the pristine state, showing good stability of the device. Taken together, the fabricated the FTTS has the advantages of simple and reliable principle, fast response, high sensitivity and good stability, making it an ideal method for detecting and simulating tactile information.

2.4. Applications of the FTTS for position detection and multi-channel information interaction

For the designed FTTS, three identical microfluidic channels with embedded liquid metal form the electrode layer in three regions. The two channels are symmetrically arranged in the lower half of the sensor, which is equivalent to the position of the finger belly of the human hand. The other channel is placed in the upper half of the sensor, which is equivalent to the fingertip position of the human hand. When the external force acted on different positions of the FTTS, the signals of the three channels showed obvious differences and independent. Based on the principle of triboelectrification, the output amplitude of each channel is mainly determined by the position of the contact and separation between the object and the sensor, which can be used to judge the position of tactile perception.

The sensor is divided into five regions (①-⑤) according to the shape of the designed electrodes. As shown in Fig. 4a-f and Supplementary materials Video S3, when an object contacts and separates from these different areas, the electrical signals of the three channels have obvious differences and show a stable regularity, that is, the larger the contact area between the object and a certain channel, the stronger the output signal of the channel. In that the effective contact area allows the tactile sensor to induce more charge, thus improving the output performance. In consequence, the effective contact position between the sensor and the object can be accurately determined according to the relative output amplitudes of the three channels. This law is consistent with the simulation of the mechanical model. The corresponding COMSOL simulation of forces applied at different positions on the FTTS are shown in Fig. 4g.

Supplementary material related to this article can be found online at [doi:10.1016/j.nanoen.2022.107324](https://doi.org/10.1016/j.nanoen.2022.107324).

The popularization of intelligent technology in the digital information age makes traditional electronic combination locks unable to meet the needs of safety, convenience and humanization, so an active encoder is urgently needed. The FTTS is integrated with the finger cover and worn on the human finger. With the help of multiple channels, three sets of signals containing cipher information could be obtained by tapping the plane continuously with different positions of the finger. By comparing with the preset code, the password authentication can be completed. Here, three kinds of ciphers are tested with the encoding method as shown in Fig. 4h. Each group of data has good differences and strong information separation (Fig. 4i-k, Fig. S7 and Supplementary materials Video S4). After integration with Bluetooth device, it can be free from the constraints of traditional cryptographic devices in fixed location. For a door lock, when the FTTS paired with the door, the password could be authenticated by tapping the trouser leg with finger without pressing the key on the door lock. With strong privacy and flexibility, so that improves the security of the password, which will definitely show broad prospects in the fields of the new generation intelligent password system.

Supplementary material related to this article can be found online at [doi:10.1016/j.nanoen.2022.107324](https://doi.org/10.1016/j.nanoen.2022.107324).

2.5. Characterization of tensile properties, stress signals and application of pulse monitoring of the FTTS

The FTTS has excellent flexibility that can accommodate various motions such as bending, stretching, and twisting (Fig. S8). Firstly, the output performance under different tensile states is systematically studied. As shown in Fig. 5a, the amplitude change of V_{OC} tends to increase with increasing stretch ratio to the FTTS. The tests are performed starting from the original state of the device, i.e., from 100% to 150%, and the output at each stretch state is tested 10 times. After stretching from 100% to 225%, the tactile sensor could still quickly return to its original state without significant output attenuation (Supplementary materials Video S5). Different from the contact-separation mode, the principle of the stretch mode of the FTTS is divergent, which is more of

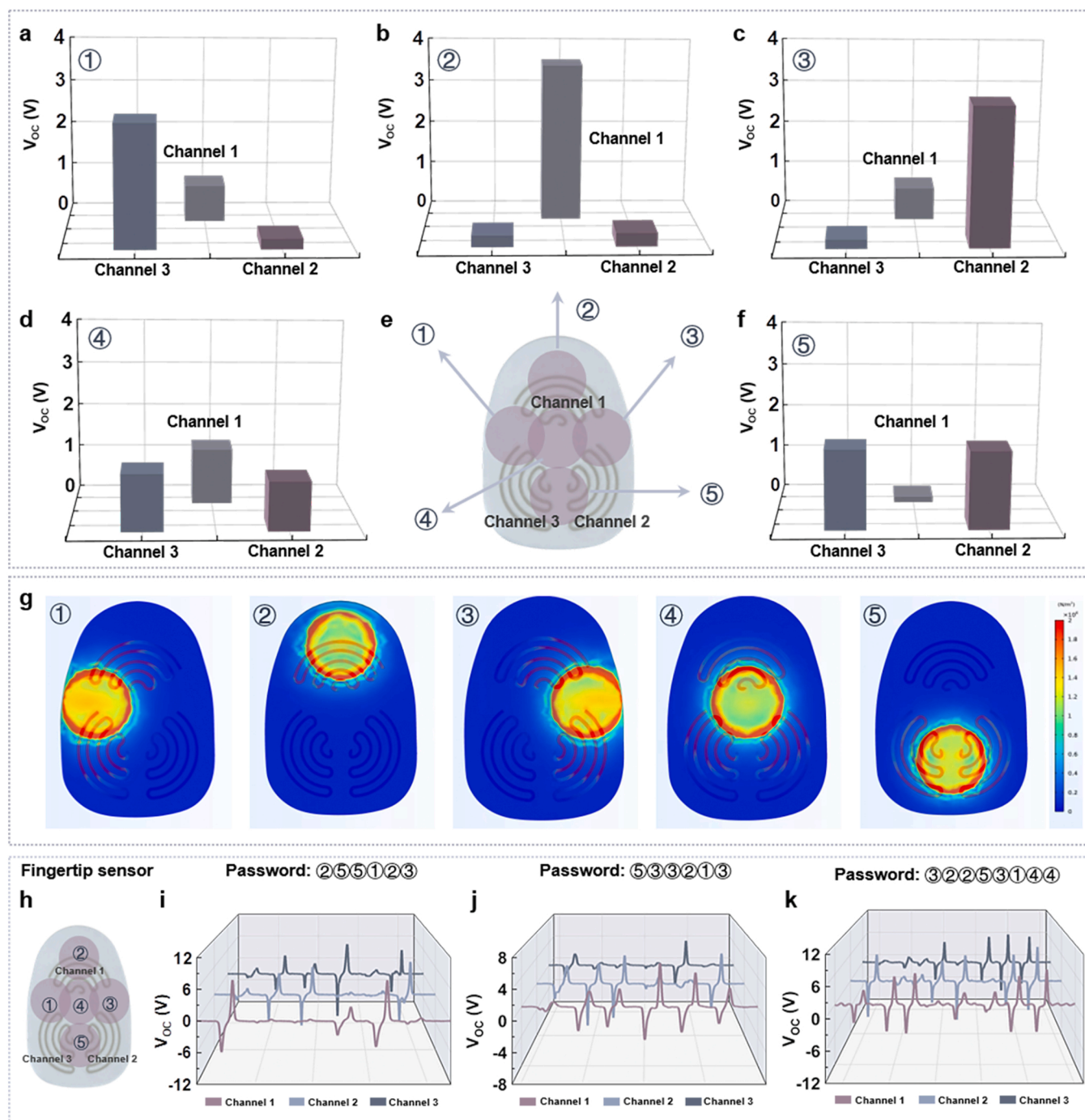


Fig. 4. Characterization of position signal and application of multi-channel information interaction of the FTTS. (a–f) Multi-channel output performance characterization for applying force to different positions of the FTTS. (g) Corresponding COMSOL simulation of forces applied at different positions on the FTTS. (h–k) Multi-channel output performance characterization for three kinds of ciphers with the encoding method in Fig. 4h enabled by the FTTS.

the internal charge transfer. As shown in Fig. 5b. In the initial state, both the silicone inner the FTTS and the surface of the liquid metal are charge-balanced, so that no electronics flow in the external circuit. When the FTTS is stretched, the contact area of silicone and liquid metal has increased, more negative charge is generated inside the silicone due to triboelectrification effect. In order to reach equilibrium, electrons flow from the liquid metal to the ground, result in output signal generating, until the FTTS is stretched to the maximum state. In the process of restoring to the initial state, the electrons flow reversely from the ground into the liquid metal in order to reach an equilibrium state. At this time, the opposite electrical signal is generated until the device is

completely restored to the original state. The corresponding COMSOL simulation schematic diagram and Video are shown in Fig. S9 and Supplementary materials Video S6.

Supplementary material related to this article can be found online at [doi:10.1016/j.nanoen.2022.107324](https://doi.org/10.1016/j.nanoen.2022.107324).

Next, the specific relationship between V_{oc} of the FTTS and the applied force is explored. Here, the signals are recorded by oscilloscope and Mark-10 system. A piece of PU with size of 2 cm × 2 cm is attached to the force detector, and repeatedly contact and separate with the TFFS at a frequency of 1 Hz. As shown in Fig. 5c, the sensor can measure the force in the range of 0–1 N well. When the applied force is greater than

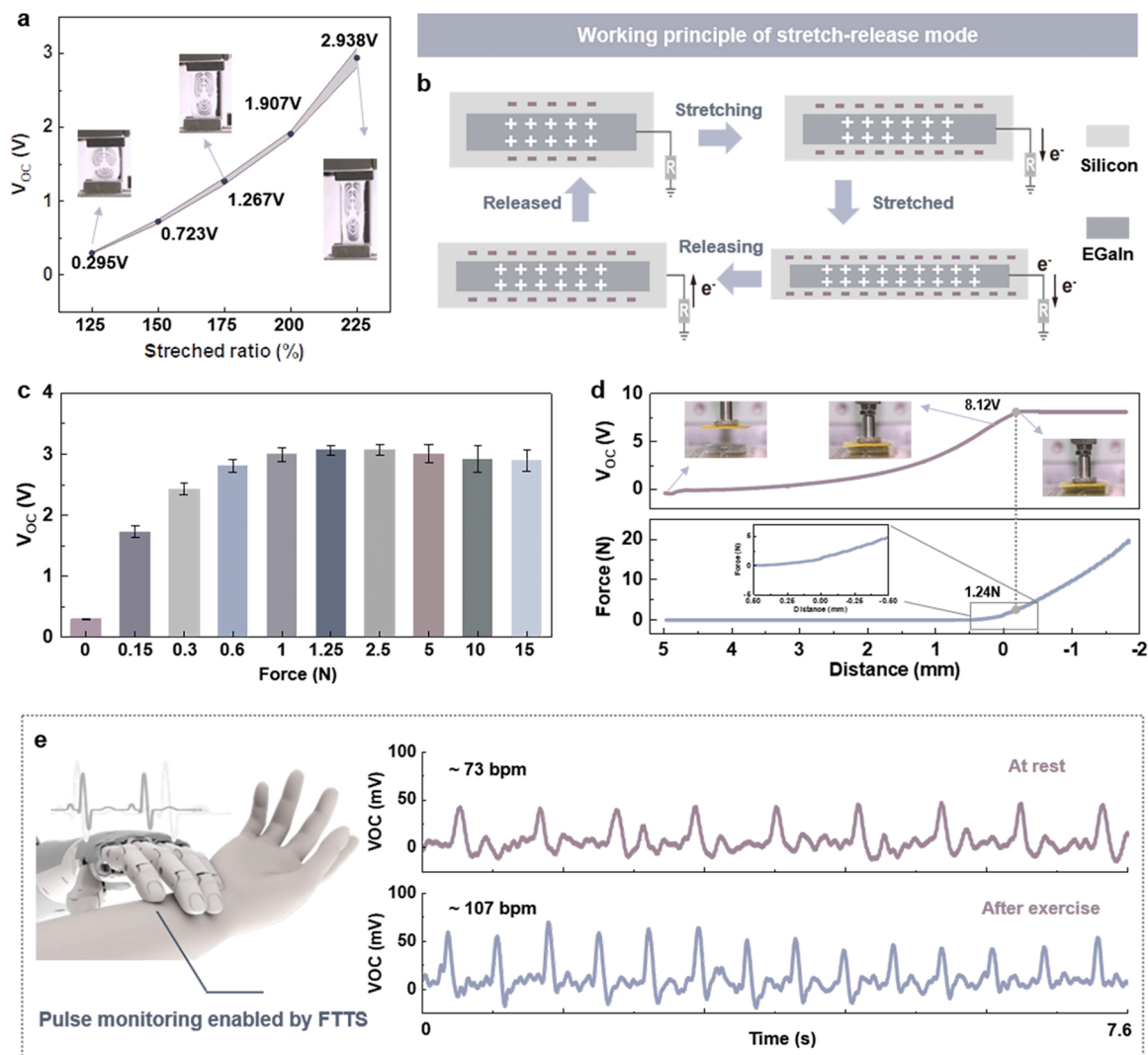


Fig. 5. Characterization of tensile properties, stress signals and application of pulse monitoring of the FTTS. (a) The amplitude of V_{OC} with different stretch ratio applied to the FTTS. (b) Working principle of the FTTS in stretch mode. (c) Output performance characterization with different force applied to the FTTS (repeatedly contact and separate with the PU, 1 Hz, recorded by oscilloscope). (d) Output performance characterization with continuous force applied to the FTTS (steady decline with PU, from 5 mm to -1.9 mm, recorded by electrometer). (e) Pulse monitoring enabled by the FTTS.

1.25 N, the output voltage measured by an oscilloscope will not change significantly. In addition, an electrometer is used to test the output voltage change when a continuous force is applied to the FTTS, and simultaneously recorded the distance traveled by the dynamometer and the force applied to the FTTS (Fig. 5d). Interestingly, when the PU on the dynamometer is 5 mm away from the FTTS surface and then moved downward continuously, the electrometer records the output signal of the non-contact state between the PU and the FTTS, which may be related to the characteristics of the triboelectric nanogenerator, which couples the triboelectrification and electrostatic induction. When they first start to contact, the trend of the output changes is consistent with that measured by the oscilloscope in Fig. 5c.

The FTTS has good response and high sensitivity to small force based on the stretch mode, which could be as an active sensor for arterial pulse detecting. Similarly, it is combined with the finger cover and worn on the finger or prosthetic limb, then placed in the right position on the wrist, the sensor can clearly detect pulse information. As shown in Fig. 5e, the pulse wave under different physiological conditions (at rest and after exercise) is intuitively displayed in real time. The V_{OC} of the FTTS has increased from 47 mV at rest to 61 mV after exercise. By analyzing the time interval between two adjacent peaks, the heart rate (beat per minute, bpm) at rest and after exercise are about 73 bpm and

107 bpm, respectively. The FTTS clearly records the characteristic peaks of peripheral arterial pulse pressure and other characteristic information, including important biomedical and physiological message for the diagnosis of cardiovascular diseases, which provides an important reference basis for the monitoring and early warning of such diseases. This sensing could endow prosthetic limbs with new functions, providing a reliable method for the realization of intelligent medical robot in the future.

3. Conclusion

In this work, we proposed a strategy to fabricated a wearable tactile sensor using EGaIn and Ecoflex for multifunctional applications. The structural design of the three separate areas with fingerprint-shaped patterned microfluidic channels and the micro structure surface of the FTTS effectively improves the sensitivity of the finger tactile sensor. The V_{OC} , I_{SC} , and Q_{SC} reaches at 15.3 V, 115.6 nA and 5.1 nC, respectively. The FTTS can respond to the force as low as 16.88 mg and also has a good signal-to-noise ratio of the output signal at 500 Hz. Due to the multi-channel design and the high sensitivity, the FTTS can detect forces applied at different locations on the sensor. Based on these features, it successfully realizes the simulation and recognition of finger password.

The fabricated FTTS is 15 mm in width, 20 mm in length and 3 mm in thick with good flexibility and stretchability. Besides, the FTTS has corresponding electrical signal output under different stretching states, and the FTTS has a good response to the force of 0–1 N. It can completely measure the pulse wave information with details, which provides an important reference basis for the monitoring and early warning of cardiovascular diseases. Based on the triboelectric effect, it can be used to identify material types due to the different ability to transfer charges between diverse materials, and the experiment also proved that the amplitude and direction of V_{OC} are different when the FTTS is exposed to various materials. It is believed that this kind of tactile sensor will have great potential in the fields of intelligent prosthetics, human-machine interactions, healthcare applications and so on.

Future work will focus on the high integration of the sensor with acquisition/control equipment, and integrate the temperature and humidity sensors, in order to realize more tactile sensing functions on intelligent prosthesis or robots.

4. Experimental section

4.1. Materials

Gallium (99.99% purity, Shanxi Zhaofeng Gallium Co., Ltd.) and indium (99.995% purity, Shanxi Zhaofeng Gallium Co., Ltd.) were prepared for the experiment. EGaIn was produced by pouring the two liquid metals in a certain proportion into a glass bottle at 180 °C and stirring them evenly for 3 h. EGaIn is sealed and stored at room temperature (about 22 °C). Before using EGaIn, it is usually washed with sodium hydroxide solution to remove the oxide. The silicone elastomer base and silicone elastomer curing agent (Ecoflex 00–30, Sooth-On, Inc.) were mixed thoroughly in a glass bottle at the ratio of 1:1. The overall size of the PTFE mold is 2 cm × 2.5 cm × 5 mm. After Computerized Numerical Control (CNC) processing, the depth of the fingerprint-shaped channel is 1.5 mm, and the depth of the microstructure portion is 1 mm.

4.2. Fabrication of the FTTS

Firstly, the prepared silicone was poured into two PTFE molds with different structures, and dried in the oven at 60 °C for 2 h. After that, the two molds were stripped and to get two membranes. Then the two membranes were bonded using the silicone adhesive and dried in the oven at 60 °C for 2 h again. Next, the prepared EGaIn was inject into the microchannel by a syringe, and the pinhole was resealed by the silicone adhesive to obtain the FTTS. The overall width and length of the FTTS are 15 mm and 20 mm, respectively.

4.3. Characterization and measurement of the FTTS

The open-circuit voltage was measured by an oscilloscope (HDO6104, Teledyne LeCroy); the short-circuit current and short-circuit charge were measured by an electrometer (6517, Keithley) and recorded by the oscilloscope (HDO6104, Teledyne LeCroy). A linear motor (E1100, LinMot) was used to apply a periodic stable force on the FTTS for periodic testing such as electrical output performance characterization and fatigue test. Tensile test of the FTTS was performed by ESM301/Mark-10 system with the tensile speed of 100 mm·min⁻¹. The investigation of the relationship between applied force and V_{OC} of TFFS was performed by the ESM301/Mark-10 system (800 mm·min⁻¹) to apply a periodic stable force on the FTTS. The simulations were implemented by COMSOL software. A platform vibrator (VT-500, YMC Piezotronics, Inc.) was employed as a high-frequency vibrator to test the response time (frequency, 500 Hz). All optical photos taken by the SLR (6D MarkII, Canon).

CRedit authorship contribution statement

Z. Li, Z. Liu and W. Rao conceived the project. X. Qu and Z. Liu designed the experiments and developed the FTTS. Z. Liu, X. Qu and Y. Liu accomplished the materials characterization. X. Qu and J. Xue completed COMSOL stimulation. W. Rao fabricated the liquid metal. X. Qu and Z. Liu performed the electrical characterization and analyzed the results. X. Qu, Z. Liu and Z. Li wrote the manuscript. All authors discussed and reviewed the manuscript.

Declaration of Competing Interest

The authors declare that they have no known competing financial interests or personal relationships that could have appeared to influence the work reported in this paper.

Acknowledgements

This work was supported by Beijing Natural Science Foundation (JQ20038 and L212010), National Natural Science Foundation of China (T2125003, 82102231 and 61875015), China Postdoctoral Science Foundation (2020M680302, 2021T140041), and the Strategic Priority Research Program of the Chinese Academy of Sciences (XDA16021101).

Appendix A. Supporting information

Supplementary data associated with this article can be found in the online version at doi:10.1016/j.nanoen.2022.107324.

References

- [1] Q.L. Hua, J.L. Sun, H.T. Liu, R.R. Bao, R.M. Yu, J.Y. Zhai, C.F. Pan, Z.L. Wang, Skin-inspired highly stretchable and conformable matrix networks for multifunctional sensing, *Nat. Commun.* 9 (2018) 244–254.
- [2] C. Bartolozzi, L. Natale, F. Nori, G. Metta, Robots with a sense of touch, *Nat. Mater.* 15 (2016) 921–925.
- [3] J. Byun, Y. Lee, J. Yoon, B. Lee, E. Oh, S. Chung, T. Lee, K.J. Cho, J. Kim, Y. Hong, Electronic skins for soft, compact, reversible assembly of wirelessly activated fully soft robots, *Sci. Robot.* 3 (2018) eaas9020.
- [4] J.A. Fishel, G.E. Loeb, Bayesian exploration for intelligent identification of textures, *Front. Neurobot.* 6 (2012) 4–23.
- [5] Y. Gao, H. Ota, E.W. Schaler, K. Chen, A. Zhao, W. Gao, H.M. Fahad, Y. Leng, A. Zheng, F. Xiong, C. Zhang, L.C. Tai, P. Zhao, R.S. Fearing, A. Javey, Wearable microfluidic diaphragm pressure sensor for health and tactile touch monitoring, *Adv. Mater.* 29 (2017), 1701985.
- [6] L. Zhang, M. Gao, R. Wang, Z. Deng, L. Gui, Stretchable pressure sensor with leakage-free liquid-metal electrodes, *Sens. (Basel)* 19 (2019), 1316–1232.
- [7] X. Qu, Y. Liu, Z. Liu, Z. Li, Assistive devices for the people with disabilities enabled by triboelectric nanogenerators, *J. Phys. Mater.* 4 (2021), 034015.
- [8] Z. Lei, Q. Wang, S. Sun, W. Zhu, P. Wu, A bioinspired mineral hydrogel as a self-healable, mechanically adaptable ionic skin for highly sensitive pressure sensing, *Adv. Mater.* 29 (2017), 1700321.
- [9] Y.C. Wang, X. Wu, D.Q. Mei, L.F. Zhu, J.N. Chen, Flexible tactile sensor array for distributed tactile sensing and slip detection in robotic hand grasping, *Sens. Actuat. a-Phys.* 297 (2019), 111512.
- [10] J. Yang, K.Y. Kwon, S. Kanetkar, R. Xing, P. Nithyanandam, Y. Li, W. Jung, W. Gong, M. Tuman, Q. Shen, M. Wang, T. Ghosh, K. Chatterjee, X. Wang, D. Zhang, T. i Kim, V.K. Truong, M.D. Dickey, Skin-inspired capacitive stress sensor with large dynamic range via bilayer liquid metal elastomers, *Adv. Mater. Technol.* (2021), 2101074.
- [11] Y. Wang, Y. Lu, D. Mei, L. Zhu, Liquid metal-based wearable tactile sensor for both temperature and contact force sensing, *IEEE Sens. J.* 21 (2021) 1694–1703.
- [12] S. Xiang, D. Liu, C. Jiang, W. Zhou, D. Ling, W. Zheng, X. Sun, X. Li, Y. Mao, C. Shan, J. Liquidens, Based wearable tactile sensor for both -powered electronic skin, *Adv. Funct. Mater.* 31 (2021), 2100940.
- [13] X. Zhao, Z. Zhang, L. Xu, F. Gao, B. Zhao, T. Ouyang, Z. Kang, Q. Liao, Y. Zhang, Fingerprint-inspired electronic skin based on triboelectric nanogenerator for fine texture recognition, *Nano Energy* 85 (2021), 106001.
- [14] G. Jin, Y. Sun, J. Geng, X. Yuan, T. Chen, H. Liu, F. Wang, L. Sun, Bioinspired soft caterpillar robot with ultra-stretchable bionic sensors based on functional liquid metal, *Nano Energy* 84 (2021), 105896.
- [15] J. Yang, W. Cheng, K. Kalantar-zadeh, Electronic skins based on liquid, *Met., P. IEEE* 107 (2019) 2168–2184.
- [16] Y. Wang, J. Jin, Y. Lu, D. Mei, 3D printing of liquid metal based tactile sensor for simultaneously sensing of temperature and forces, *Int. J. Smart Nano Mater.* 12 (2021) 269–285.

- [17] P. Yong-Lae, C. Bor-Rong, R.J. Wood, Design and fabrication of soft artificial skin using embedded microchannels and liquid conductors, *IEEE Sens. J.* 12 (2012) 2711–2718.
- [18] M.A. Abd, M. Al-Saidi, M. Lin, G. Liddle, E.D. Engeberg, In surface feature recognition and grasped object slip prevention with a liquid metal tactile sensor for a prosthetic hand, *BioRob* (2020).
- [19] H. Feng, C. Zhao, P. Tan, R. Liu, X. Chen, Z. Li, Nanogenerator for biomedical applications, *Adv. Healthc. Mater.* 7 (2018), e1701298.
- [20] Z. Liu, Y. Ma, H. Ouyang, B.J. Shi, N. Li, D.J. Jiang, F. Xie, D. Qu, Y. Zou, Y. Huang, H. Li, C.C. Zhao, P.C. Tan, M. Yu, Y.B. Fan, H. Zhang, Z.L. Wang, Z. Li, Transcatheter self-powered ultrasensitive endocardial pressure sensor, *Adv. Funct. Mater.* 29 (2019), 1807560.
- [21] Y. Yang, L.L. Xu, D.J. Jiang, B.Z. Chen, R.Z. Luo, Z. Liu, X.C. Qu, C. Wang, Y. Z. Shan, Y. Cui, H. Zheng, Z.W. Wang, Z.L. Wang, X.D. Guo, Z. Li, Self-powered controllable transdermal drug delivery system, *Adv. Funct. Mater.* 31 (2021), 2104092.
- [22] G. Yao, L. Kang, C.C. Li, S.H. Chen, Q. Wang, J.Z. Yang, Y. Long, J. Li, K.N. Zhao, W.N. Xu, W.B. Cai, Y. Lin, X.D. Wang, A self-powered implantable and bioresorbable electrostimulation device for biofeedback bone fracture healing, *Proc. Natl. Acad. Sci. USA* 118 (2021), e2100772118.
- [23] Q. Zheng, Q. Tang, Z.L. Wang, Z. Li, Self-powered cardiovascular electronic devices and systems, *Nat. Rev. Cardiol.* 18 (2021) 7–21.
- [24] Y. Zou, P. Tan, B. Shi, H. Ouyang, D. Jiang, Z. Liu, H. Li, M. Yu, C. Wang, X. Qu, L. Zhao, Y. Fan, Z.L. Wang, Z. Li, A bionic stretchable nanogenerator for underwater sensing and energy harvesting, *Nat. Commun.* 10 (2019) 2695–2704.
- [25] T. Chen, Q.F. Shi, M.L. Zhu, T.Y.Y. He, L.N. Sun, L. Yang, C. Lee, Triboelectric self-powered wearable flexible patch as 3D motion control interface for robotic manipulator, *ACS Nano* 12 (2018) 11561–11571.
- [26] T. Jin, Z.D. Sun, L. Li, Q. Zhang, M.L. Zhu, Z.X. Zhang, G.J. Yuan, T. Chen, Y. Z. Tian, X.Y. Hou, C. Lee, Triboelectric nanogenerator sensors for soft robotics aiming at digital twin applications, *Nat. Commun.* 11 (2020) 5381–5392.
- [27] M.L. Zhu, Z.D. Sun, T. Chen, C.K. Lee, Low cost exoskeleton manipulator using bidirectional triboelectric sensors enhanced multiple degree of freedom sensory system, *Nat. Commun.* 12 (2021) 2692–2707.
- [28] Z. Liu, Q. Zheng, Y. Shi, L. Xu, Y. Zou, D. Jiang, B. Shi, X. Qu, H. Li, H. Ouyang, R. Liu, Y. Wu, Y. Fan, Z. Li, Flexible and stretchable dual mode nanogenerator for rehabilitation monitoring and information interaction, *J. Mater. Chem. B* 8 (2020) 3647–3654.
- [29] X.J. Pu, H.Y. Guo, J. Chen, X. Wang, Y. Xi, C.G. Hu, Z.L. Wang, Eye motion triggered self-powered mechnosensational communication system using triboelectric nanogenerator, *Sci. Adv.* 3 (2017), e1700694.
- [30] X. Qu, X. Ma, B. Shi, H. Li, L. Zheng, C. Wang, Z. Liu, Y. Fan, X. Chen, Z. Li, Z. L. Wang, Refreshable braille display system based on triboelectric nanogenerator and dielectric elastomer, *Adv. Funct. Mater.* 31 (2020), 2006612.
- [31] C. Wang, X. Qu, Q. Zheng, Y. Liu, P. Tan, B. Shi, H. Ouyang, S. Chao, Y. Zou, C. Zhao, Z. Liu, Y. Li, Z. Li, Stretchable, self-healing, and skin-mounted active sensor for multipoint muscle function assessment, *ACS Nano* 15 (2021) 10130–10140.
- [32] Y. Wu, Y. Li, Y. Zou, W. Rao, Y. Gai, J. Xue, L. Wu, X. Qu, Y. Liu, G. Xu, L. Xu, Z. Liu, Z. Li, A multi-mode triboelectric nanogenerator for energy harvesting and biomedical monitoring, *Nano Energy* 92 (2022), 106715.
- [33] Y. Cao, Y. Yang, X. Qu, B. Shi, L. Xu, J. Xue, C. Wang, Y. Bai, Y. Gai, D. Luo, Z. Li, A self-powered triboelectric hybrid coder for human-machine interaction, *Small Methods* (2022), e2101529.
- [34] C. Chen, Z. Wen, J.H. Shi, X.H. Jian, P.Y. Li, J.T.W. Yeow, X.H. Sun, Micro triboelectric ultrasonic device for acoustic energy transfer and signal communication, *Nat. Commun.* 11 (2020) 4143–4151.
- [35] R. Hinchet, H.J. Yoon, H. Ryu, M.K. Kim, E.K. Choi, D.S. Kim, S.W. Kim, Transcutaneous ultrasound energy harvesting using capacitive triboelectric technology, *Science* 365 (2019) 491–494.
- [36] T. He, X. Guo, C. Lee, Flourishing energy harvesters for future body sensor network: from single to multiple energy sources, *iScience* 24 (2021), 101934.
- [37] Z. Sun, M. Zhu, C. Lee, Prog. Triboelectric Hum. Interfaces (HMIs)-Mov. Smart Gloves AI/Haptic Enabled HMI 5G/IoT Era 1 2021 81 120.
- [38] F. Wen, Z. Zhang, T. He, C. Lee, AI enabled sign language recognition and VR space bidirectional communication using triboelectric smart glove, *Nat. Commun.* 12 (2021) 5378–5390.



Xuecheng Qu received his B.S. degree in Electric Engineering and Automotive from University of Jinan in 2017. He is currently pursuing the Ph.D degree with the Department of Biophysics, Beijing Institute of Nanoenergy and Nanosystems, Chinese Academy of Sciences. His current interests include self-powered sensors, systems and applications based on nanogenerators.



Jiangtao Xue received his B.S. degree from Beijing University of Technology in 2016. He is currently a Ph.D. student at the Institute of Engineering Medicine, Beijing Institute of Technology. His research interests mainly focus on nanogenerators and wearable electronics.



Ying Liu received her B.S. degree in Polymer Material and Engineering from Tianjin University of Science and Technology in 2019. She is currently pursuing the M.D. degree with the Department of Biophysics, Beijing Institute of Nanoenergy and Nanosystems, Chinese Academy of Sciences. Her current interests include stretchable conductive materials and flexible self-powered electronics.



Wei Rao received her Ph.D. from Technical Institute of Physics and Chemistry, Chinese Academy of Sciences in 2009, and Bachelor's and Master's Degree from Harbin Institute of Technology in 2003 and 2006, respectively. Currently, she is a Professor in the Technical Institute of Physics and Chemistry (TIPC), Chinese Academy of Sciences. Her research interests include liquid metal materials and technology, cryo-biomedicine and nanosensitizers.



Zhuo Liu received his Ph.D. in Biomedical Engineering from Beihang University in 2020. He is currently doing postdoctoral research at Beijing Advanced Innovation Centre for Biomedical Engineering, Beihang University. His research interests are focusing on self-powered biomedical systems and measurement of cell traction force.



Zhou Li received his Ph.D. from Peking University in Department of Biomedical Engineering in 2010, and Bachelor's Degree from Wuhan University in 2004. He joined School of Biological Science and Medical Engineering of Beihang University in 2010 as an Associate Professor. Currently, he is a Professor in Beijing Institute of Nanoenergy and Nanosystems, Chinese Academy of Sciences. His research interests include nanogenerators, in vivo energy harvesters, self-powered medical devices, and biosensors.